Arch. Metall. Mater. **68** (2023), 3, 1115-1120

DOI: https://doi.org/10.24425/amm.2023.145482

I. MATUŁA[1*], G. DERCZ[1*], K. PRUSIK[1], M. SZKLARSKA[1], A. KAZEK-KĘSIK[2], W. SIMKA[2], E. SUDOŁ[3]

SYNTHESIS OF Ti-Nb-Zr ALLOYS COMBINED POWDER METALLURGY AND ARC MELTING METHODS

Scientists and medics are still searching for new metallic materials that can be used in medicine, e.g., as material for implants. The following article proposes materials based on titanium with vital elements prepared by combined powder metallurgy and arc melting methods. Four compositions of Ti-28Ta-9Nb, Ti-28Ta-19Nb, Ti-28Ta-9Zr and Ti-28Ta-19Zr (wt.%) have been prepared. The tested material was thoroughly analyzed by X-ray diffraction and scanning electron microscopy. Qualitative phase analysis using X-ray diffraction showed the presence of two phases, α' and β titanium. In addition, a microhardness test was conducted, and the material was characterized in terms of corrosion properties. It was found that the corrosion resistance decreases with an increase of the β phase presence.

Keywords: Titanium-based alloys; biomaterials; arc-melting; structure; corrosion

1. Introduction

Titanium and its alloys have many advantages compared to the other metallic biomaterials, such as high strength, low density, excellent corrosion resistance in various body fluid environments, and biocompatibility. Additionally, the titanium has also lower Young's modulus in comparison to other metallic materials [1-4]. The main problem with commercial used alloy for implants is presence of aluminum and vanadium. Unfortunately, in literature are increasing reports of the toxicity of the aforementioned elements, which can affect nerve cell damage and bone softening. Currently, intensive research work is underway on titanium alloys, in which aluminum and vanadium are replaced by less toxic elements like tantalum, zirconium and niobium [1,5-9]. Zirconium have been deeply investigated as biomedical materials and belongs to the group of vital elements. Zr revealed low cytotoxicity, excellent biocompatibility and very high corrosion resistance [2,10]. Titanium and Zirconium belong to the same group in periodic table. Moreover, the phase diagram revealed the complete solution and the same crystal structure of both elements [11]. Niobium is an element that is well tolerated by the human body, exhibit very good biocompatibility and corrosion resistance. Additionally, the Nb is β-stabilizer in titanium alloy, already the presence of 25 wt.% of the Nb supports the presence of the phase β [11-14]. Tantalum is one of the most promising element additives to titanium alloy in term of high biocompatibility. The addition of tantalum improve the corrosion resistance and strength of material compare to pure titanium [2,15,16]. Titanium, zirconium, tantalum and niobium are not carcinogenic, genotoxic or mutagenic [2].

The main aim was production of new biomedical alloys from the Ti-28Ta-X system with variable content of Zr and Nb elements by combination of homogenization by powder metallurgy and arc melting. The as-prepared material was thoroughly analyzed by X-ray diffraction, scanning electron microscopy, microhardness measurement and corrosion resistance.

2. Materials and Methods

Commercially available powders of Ti (Atlantic Equipment Engineers (AEE); purity 99.7%), Ta (Sigma Aldrich; purity 99.9%; particle size <300 μm), Nb (Atlantic Equipment Engineers (AEE), purity 99.8%, particle size <5 μm), Zr (Atlantic Equipment Engineers (AEE); purity 99.5%; particle size <300 μm) were used to prepare four chemical compositions: Ti-28Ta-9Nb, Ti-28Ta-19Nb, Ti-28Ta-9Zr and Ti-28Ta-19Zr (wt.%). The first step of material preparation was homogenization in planetary ball-mill Fritch Pulverisette 7 premium line with parameters: rotation speed was 200 rpm, time was 24 hours, the weight ratio of balls to the material was 10:1 and the process were carried out in argon atmosphere. In the next step

[1] UNIVERSITY OF SILESIA IN KATOWICE, INSTITUTE OF MATERIALS ENGINEERING, 75 PUŁKU PIECHOTY STR., 1 A, 41-500 CHORZÓW, POLAND
[2] SILESIAN UNIVERSITY OF TECHNOLOGY, FACULTY OF CHEMISTRY, 6 B. KRZYWOUSTEGO STR., 44-100 GLIWICE, POLAND
[3] GRADUATE, INSTITUTE OF MATERIALS ENGINEERING, UNIVERSITY OF SILESIA IN KATOWICE, 75 PUŁKU PIECHOTY STREET 1 A, 41-500 CHORZÓW, POLAND

* Corresponding authors: Izabela.matula@us.edu.pl; grzegorz.dercz@us.edu.pl

from the powder were prepared green compacts by cold isostatic pressing under 1000 MPa. The second stage of material preparation was remelting by the vacuum arc melting (VAM) technique in an Ar-protective atmosphere under the 1.2 bar pressure. Before melting the alloys, a high-purity Ti-getter was used to remove the residual gases from a chamber. To homogenize, the obtained by VAR buttons were flipped over and re-melted five times for the 60 s each time. In the third and final step, the samples were subjected to homogenization in the furnace at 1000°C for 24 hours.

The phase composition were analyzed by X-ray diffraction method (XRD), using a Phillips X-ray X'Pert diffractometer having a lamp with a copper anode (CuKα – λ = 1.54178 Å). The registration of diffractograms were performed with 40kV acceleration voltage with step-scan 0.04°. The Rietveld analysis was applied and performed by DBWS-9807 program [17]. The R_{wp} (weighted-pattern factor) and S (goodness-of-fit) parameters were used as numerical criteria for the quality of the fit of the calculated to experimental diffraction data [18,19].

The microstructure of samples were observed using the optic microscope (OM) Olympus GX-51 and scanning electron microscope (SEM) JSM 6480. Additionally, were performed chemical composition analyses using an energy dispersive X-ray spectroscopy detector (EDS). The samples for observation were prepared by griding, polishing and eatching.

As the first look on mechanical properties were the microhardness measurements. The Vickers microhardness measurement was conducted on Wolpert 401MVD tester with the load of 500 N for a loading time of 10 s.

The corrosion resistance of titanium alloys were conducted using a PARSTAT 4000 potentiostat (AMETEK). The measuring apparatus consisted of a thermostated electrolytic cell and three electrodes: working electrode (WE), auxiliary platinum electrode (CE) and Haber-Luggin capillary with reference electrode (RE) – saturated calomel electrode – SEC. Corrosion resistance measurements were carried out at 37°C in Ringer's solution. During the measurements, the following were determined: open circuit potential E_{OC} [mV], the polarization curve in the E_{OC} potential range from –20 mV to +20 mV, (dE/dt = 1 mV s^{-1}) and cyclic voltammetry curve in the E_{OC} potential range from –0.1 mV to 3 V. The parameters of corrosion potential, E_{COR}, mV; and polarization resistance R_p, Ω cm^2 were determined from the polarization curves. The corrosion current density was recalculated according to the Stearn-Gear's method

$$j_{CORR} = \frac{\beta_a \beta_b}{2.303(\beta_a + \beta_b) R_p} = \frac{B}{R_p},\ \mathrm{A\,cm^{-2}}$$

Where: B is the Stern-Gear constant [V], β_a and β_b are the slopes of the anodic and cathodic Tafel sections, respectively [V], and R_p is the polarization resistance at the corrosion potential [$\Omega \cdot cm^2$].

The value of polarization resistance R_p was calculated according to the relation:

$$R_p = \left(\frac{\partial \cdot E}{\partial j} \right)_{j=0, dE/dt \to 0},\ \Omega \cdot \mathrm{cm}^2$$

3. Results and Discussion

Qualitative phase analysis revealed the presence of two phases α' and β of titanium in all samples (Fig. 1 and 2). It should be noted that the β phase is dominant for all samples. The disturbances in intensity of the diffraction lines observed in the diffractogram of samples were caused presence of a large grain, what was confirmed by microscopic observations. Detailed analysis by the Rietveld method allowed to determine the structural parameters and perform the quantitative phase analysis (TABLE 1 and 2). For Ti-28Ta-9Nb and Ti-28Ta-19Nb sample were

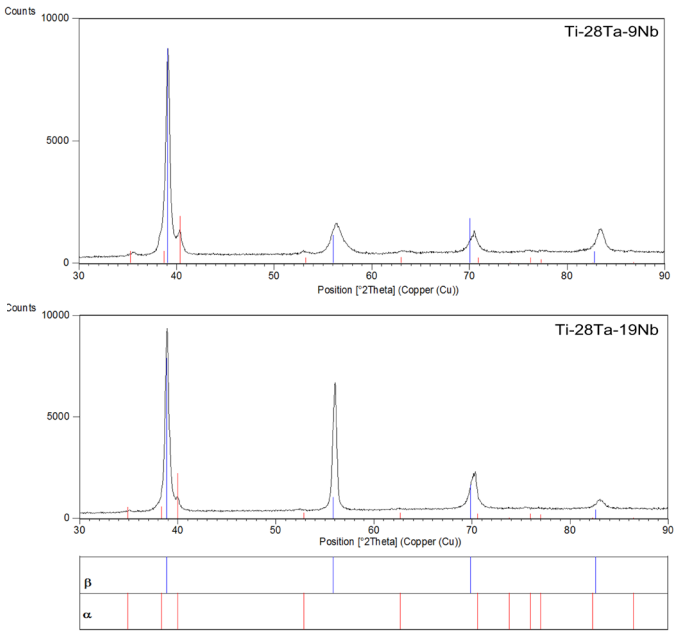

Fig. 1. XRD patterns of Ti-28Ta-9Nb and Ti-28Ta-19Nb sample

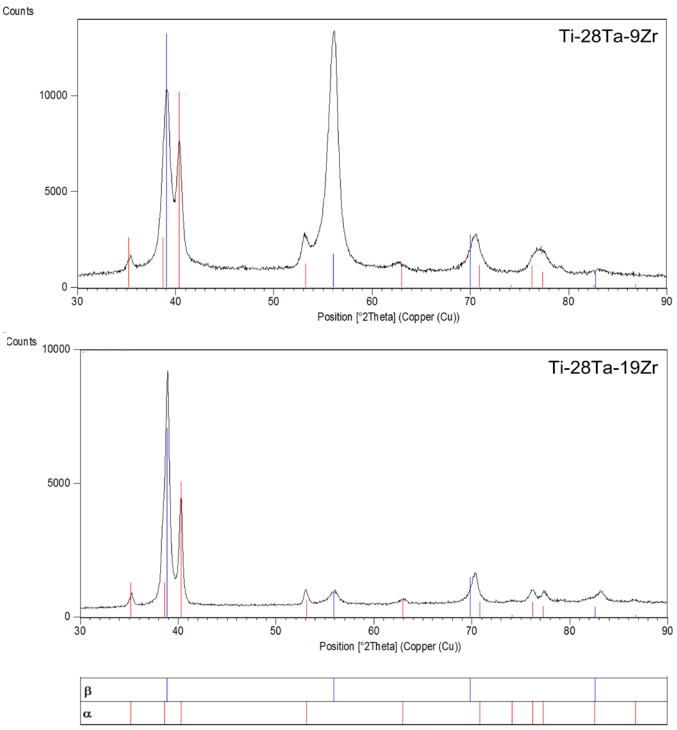

Fig. 2. XRD patterns of Ti-28Ta-9Zr and Ti-28Ta-19Zr sample

observed content of 93.6 and 96.4 wt.% β-Ti, respectively. C.M. Lee et. Al. [20], shown that in the binary system Ti-Nb demand at least 30 wt. % of Nb to obtain β-Ti. Additionally, in the Ti-Ta binary system, the minimum content of Ta to obtain β-Ti alloy is 55 wt. % [20,21]. The combination of the presence of tantalum and niobium makes it possible to obtain a high beta content (more than 90%). In contrast, increasing the niobium content by 10% by weight did not affect the β-Ti phase content significantly. For Ti-28Ta-9Zr and Ti-28Ta-19Zr composition were observed 81.3 and 64.1 wt.% β-Ti, respectively (TABLE 1). Higher zirconium content by weight resulted in lower beta content. In this case only tantalum is responsible of β phase formation, because zirconium is a neutral element, indeed stabilizes the α-Ti phase [10,22-26]. A detailed the Rietveld analysis allowed to observation of changes in lattice parameters (TABLE 2). In case Ti-28Ta-9Nb and Ti-28Ta-19Nb composition a slight increase in the values of lattice parameters for α' phase was found with a simultaneous, slight expansion of the elementary cell for the β phase. In case Ti-28Ta-9Zr and Ti-28Ta-19Zr composition an increase in the values of the lattice parameters for the α phase was found, at the same time the a_0 value for the β phase increased. The atomic radius of Ta (1.45 Å) and Nb (1.45 Å) are close to atomic radius of Ti (1.40 Å), negligible cause an increase in the lattice parameters of the newly formed β phase. The observed lattice expansions of the α' and β phases observed for the samples with Zr are related to the fact of a larger atomic radius Zr (1.55Å) [26,27].

TABLE 1

Changes in quantitative phase composition for all samples

Phase	Sample			
	Ti-28Ta-9Nb	Ti-28Ta-19Nb	Ti-28Ta-9Zr	Ti-28Ta-19Zr
α	6.4(4)	3.6(3)	18.7(4)	35.9(3)
β	93.6(8)	96.4(8)	81.3(8)	64.1(8)

Fig. 3 show the optic microscope photos and revealed the needle-like microstructure for all samples however, differing in distribution and size. The sample Ti-28Ta-19Zr were observed distinctly different microstructure, whit increase of Zr content increase the size of grains. In the case of composition with Nb were observed smaller needle-like grains with increase of the niobium content, thereby a smaller participation of α' phase. The increasing of the niobium content causes the dendritic structure to become less pronounced and the needle-like areas to disappear [20,28].

Fig. 4 present SEM photographs of all samples and show bi-phase nature of samples. In case of composition with Nb were

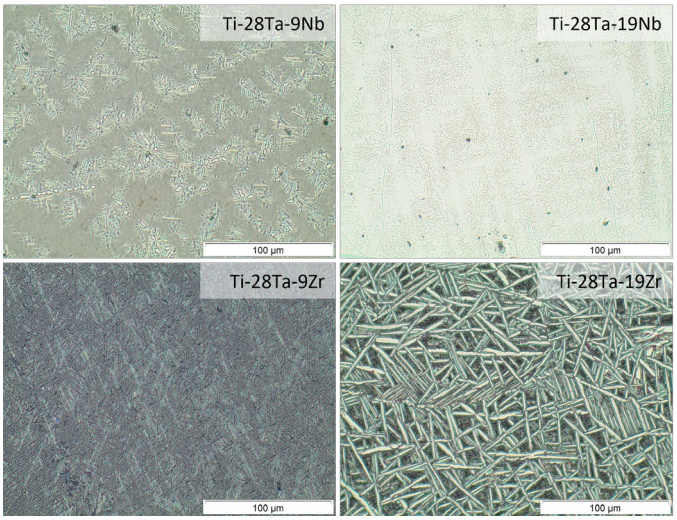

Fig. 3. OM images of Ti-28Ta-9Nb, Ti-28Ta-19Nb, Ti-28Ta-9Zr and Ti-28Ta-19Zr (wt.%) samples (scale bar 100 µm)

clearly observed grains boundaries. It also confirmed the presence of finer needles inside the grain for the sample with higher Nb content. In contrast, images for the samples Ti-28Ta-9Zr and Ti-28Ta-19Zr revealed significantly finer needles. Analysis of the element distributions (Fig. 5) revealed a higher concentration of titanium in darker needles, with simultaneous lower concentration of tantalum. It can be explain by the presence of α phase in the observed area. Zirconium is homogenously distributed throughout the sample.

The first look on mechanical properties were microhardness measurement. The microhardness values are 439 HV0.5 for Ti-28Ta-9Nb, 313 HV0.5 for Ti-28Ta-19Nb, 469 HV0.5 for Ti-28Ta-9Zr and 449 HV0.5 for Ti-28Ta-19Zr. Generally, the values were highest for sample with zirconium in comparison to samples with Nb. However, there are no significant differences between the samples with zirconium. In case of Ti-28Ta-9Nb and Ti-28Ta-19Nb, alloys similary as X. Tang et al. [29] were observed decrease of microhardness measurement with increase of Nb content.

TABLE 3 summarizes the results obtained from corrosion resistance tests for the titanium alloys tested in Ringer's solution. The open circute potential for all tested surfaces was measured in Ringer's solution for 60 minutes and it is presented in Fig. 6. The value of E_{OC} registered for all tested samples was similar and ranged from –276.3 mV to –258.8 mV. The tested samples revealed differences in their corrosion potential (E_{COR}), polarization resistance (R_p) and corrosion current density (j_{COR}). The

TABLE 2

Unit-cell parameters of α and β phases of all samples

Phase	Unit-cell parameter [nm]	ICDD	Sample			
			Ti-28Ta-9Nb	Ti-28Ta-19Nb	Ti-28Ta-9Zr	Ti-28Ta-19Zr
α'	a_0	0.2970	0.2975(2)	0.2981(2)	0.2958(2)	0.2981(2)
	c_0	0.4720	0.4658(4)	0.4671(4)	0.4703(4)	0.4712(4)
β	a_0	0.3307	0.3289(3)	0.3299(3)	0.3293 (3)	0.3304(3)

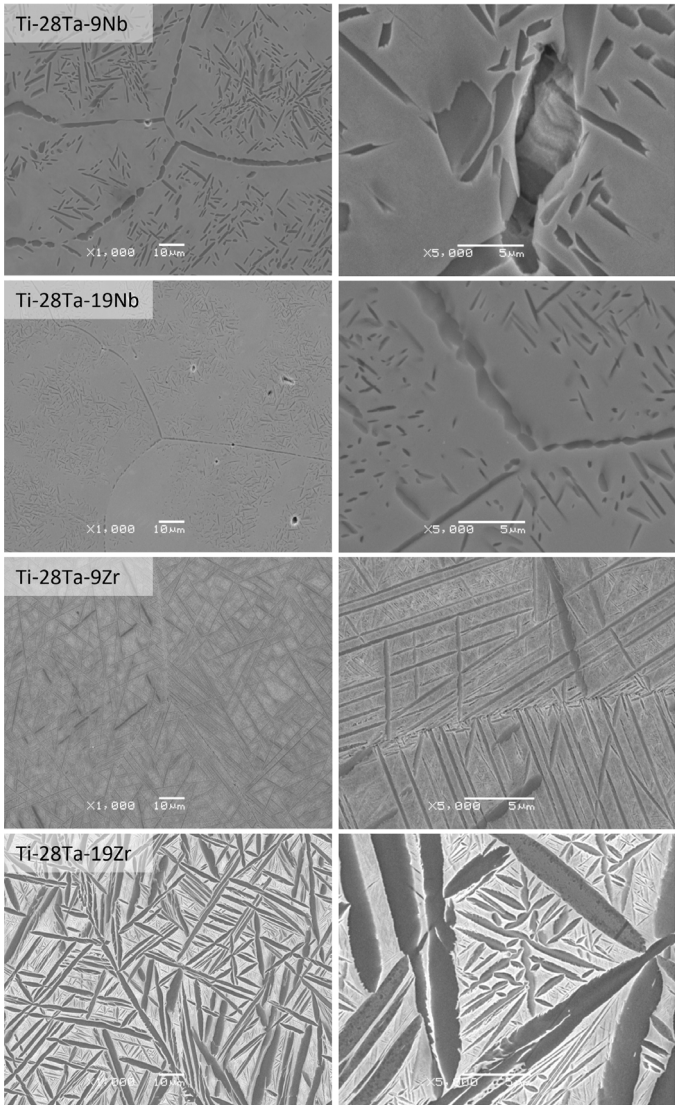

Fig. 4. SEM images of Ti-28Ta-9Nb, Ti-28Ta-19Nb, Ti-28Ta-9Zr and Ti-28Ta-19Zr (wt.%) samples (scale bar 10 μm on the left, 5 μm on the right)

TABLE 3

Results of corrosion resistance tests of titanium alloy samples

Sample	E_{OC}, mV	E_{COR}, mV	Rp, Ω cm^2	j_{COR} A cm^{-2}	Tafel slope, V	
					β_a	β_a
N1	–258.9	–275.5	$1.0 \cdot 10^7$	$4.1 \cdot 10^{-8}$	0.432	0.310
N2	–270.9	–274.2	$5.5 \cdot 10^6$	$7.8 \cdot 10^{-8}$	0.145	0.351
Z1	–276.3	–285.1	$9.6 \cdot 10^6$	$4.5 \cdot 10^{-8}$	0.152	0.308
Z2	–267.4	–264.7	$9.8 \cdot 10^6$	$4.4 \cdot 10^{-8}$	0.122	0.124

Ti-28Ta-9Nb alloy sample had the highest polarization resistance value. However, Ti-28Ta-9Nb sample show a slightly lower value of corrosion current density $j_{COR} = 4.1 \cdot 10^{-8}$ A cm^{-2}. The voltammetric curves registered for the investigated titanium alloy samples are shown in Fig. 8. The shape of the voltammetric curves is significantly affected by the surface morphology, what is clearly visible in case of Ti-28Ta-19Nb sample. For all samples, an increase in current density above the potential of 0.4 V vs. SEC was registered. However, a rapid increase in current density was observed at a potential of 1.2 V vs. SEC and reached the maximum at a potential value of about 2.5 V. The shape of the voltammetric curves indicates the formation of oxide layers. On the surface of titanium alloys, titanium oxides such as TiOOH, Ti_2O_3 are formed, then at a potential above 0.1 V, Ti^{3+} ions are oxidized to Ti^{4+} forming a stable TiO_2 phase. The recorded signal at a potential of 1.4-2 V vs. SCE indicates that the electrode is oxidized and oxides, including non-stoichiometric oxides, are formed on the surface.

The sample Ti-28Ta-9Nb revealed the highest corrosion resistance and the Ti-28Ta-19Nb show the lowest corrosion resistance compared to the rest of the samples. Samples Ti-28Ta-9Zr and Ti-28Ta-19Zr have approximate values to sample Ti-28Ta-9Nb.

3. Conclusion

Based on the obtained results in the research the following conclusion can be drawn:

1. The combination of powder metallurgy method and arc melting allow for successfully production of Ti-28Ta-9Nb, Ti-28Ta-19Nb, Ti-28Ta-9Zr and Ti-28Ta-19Zr (wt.%) alloys.
2. Qualitative phase analysis performed using X-ray diffraction showed bi-phase structure with the presence of two phases, α' and β titanium.
3. The correlation of the dependence of the chemical composition of the Ti-28Ta-19Nb (wt.%) material and the phase composition and properties of the obtained material is visible. The corrosion resistance decreases with an increase in the proportion of the β phase.
4. It was found that in the Ti-28Ta-9Nb, Ti-28Ta-19Nb alloys were observed a commasification of titanium at the grain boundaries, while the β-creative elements (Nb and Ta) locate inside the grains. the β phase.

REFERENCES

[1] A.M. Khorasani, M. Goldberg, E.H. Doeven, G. Littlefair, Titanium in Biomedical Applications-Properties and Fabrication: A Review, J. Biomater. Tissue Eng. **5**, 593-619 (2015). DOI: https://doi.org/10.1166/jbt.2015.1361

[2] Y. Li, C. Yang, H. Zhao, S. Qu, X. Li, Y. Li, New developments of ti-based alloys for biomedical applications, Materials **7**, 1709-1800 (2014). DOI: https://doi.org/10.3390/ma7031709

[3] M. Niinomi, M. Nakai, J. Hieda, Development of new metallic alloys for biomedical applications, Acta Biomater. **8**, 3888-3903 (2012). DOI: https://doi.org/10.1016/j.actbio.2012.06.037

[4] M. Long, H.J. Rack, Titanium alloys in total joint replacement – a materials science perspective, Biomaterials **19** (18), 1621-1639 (1998). DOI: https://doi.org/10.1016/S0142-9612(97)00146-4

[5] K.J. Bozic, S.M. Kurtz, E. Lau, K. Ong, D.T.P. Vail, D.J. Berry, The epidemiology of revision total hip arthroplasty in the

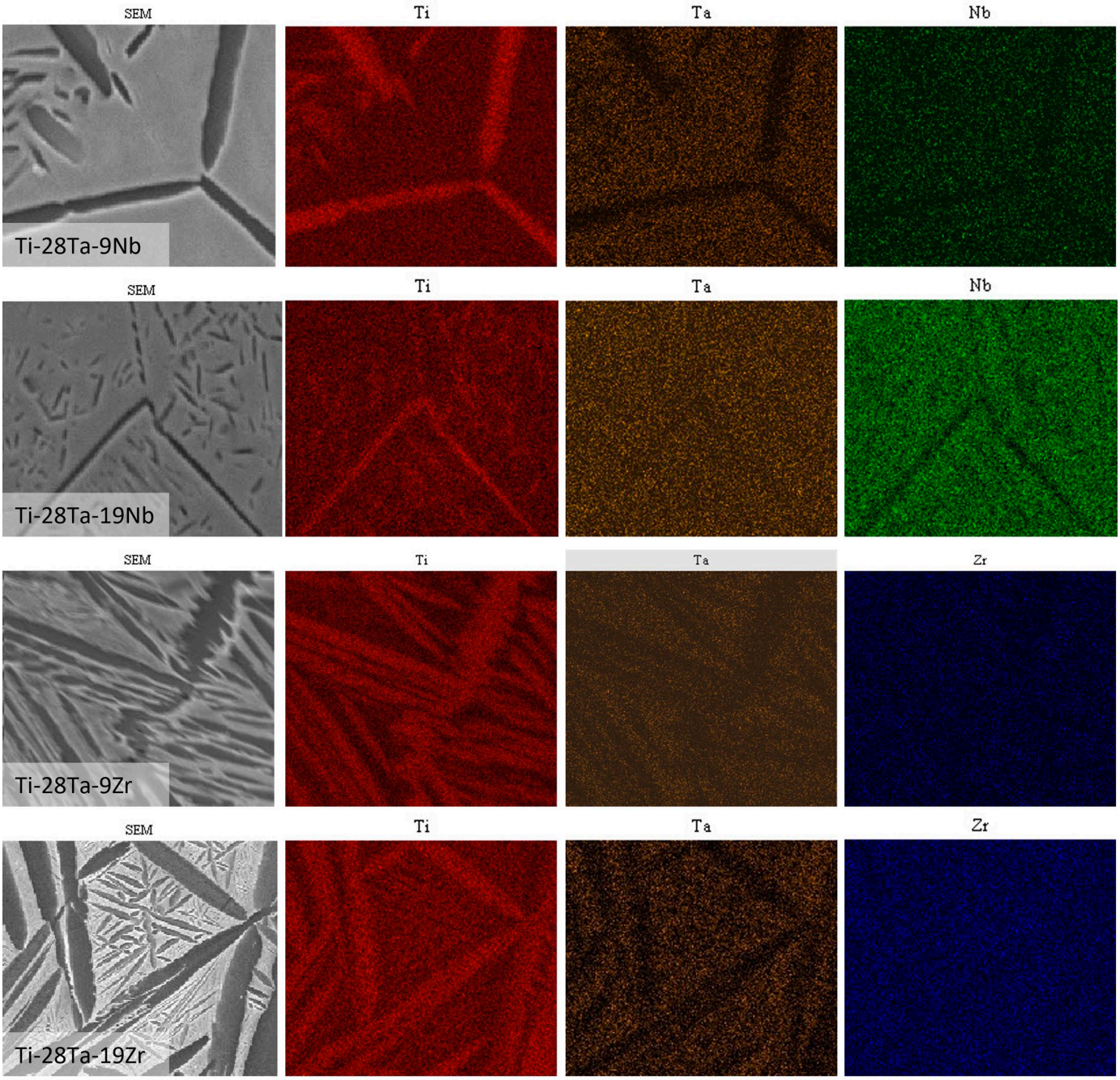

Fig. 5. Map of element distribution for Ti-28Ta-9Nb, Ti-28Ta-19Nb, Ti-28Ta-9Zr and Ti-28Ta-19Zr (wt.%); Ti – red, Ta – orange, Nb – green, Zr – blue

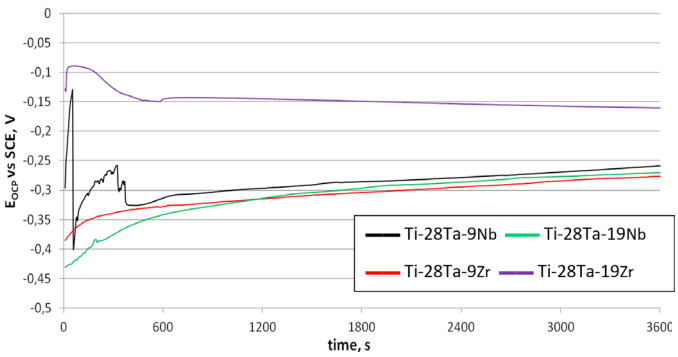

Fig. 6. Open circuit potential as a function of time for the Ti-28Ta-9Nb, Ti-28Ta-19Nb, Ti-28Ta-9Zr and Ti-28Ta-19Zr (wt.%)

United States, J. Bone Joint Surg. Am. **91**, 128-133 (2009). DOI: https://doi.org/10.2106/JBJS.H.00155

[6] J. Willis, S. Li, S.J. Crean, F.N. Barrak, Is titanium alloy Ti-6Al-4 V cytotoxic to gingival fibroblasts – A systematic review, Clin. Exp. Dent. Res. **7**, 1037-1044 (2021). DOI: https://doi.org/10.1002/CRE2.444

[7] K. Wang, The use of titanium for medical applications in the USA, Materials Science and Engineering: A **213** (1-2), 134-137 (1996). DOI: https://doi.org/10.1016/0921-5093(96)10243-4

[8] S. Rao, T. Ushida, T. Tateishi, Y. Okazaki, S. Asao, Effect of Ti, Al, and V ions on the relative growth rate of fibroblasts (L929) and osteoblasts (MC3T3-E1) cells, Biomed. Mater. Eng. **6**, 79-86 (1996). DOI: https://doi.org/10.3233/BME-1996-6202

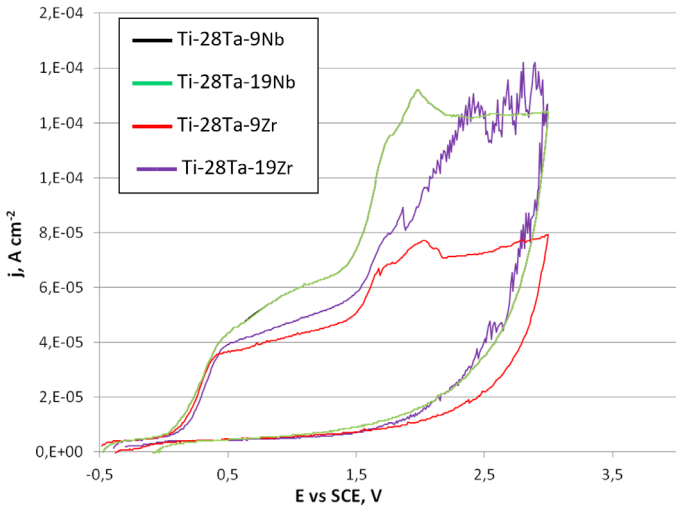

Fig. 8. Voltammetric curves for samples Ti-28Ta-9Nb, Ti-28Ta-19Nb, Ti-28Ta-9Zr and Ti-28Ta-19Zr (wt.%)

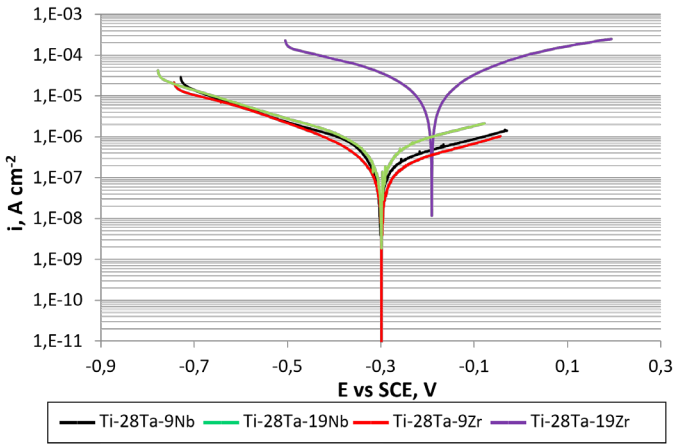

Fig. 7. Polarization curves for samples Ti-28Ta-9Nb, Ti-28Ta-19Nb, Ti-28Ta-9Zr and Ti-28Ta-19Zr (wt.%)

[9] K.L. Wapner, Implications of metallic corrosion in total knee arthroplasty, Clin. Orthop. Relat. Res. **271**, 12-20 (1991).

[10] I. Matuła, G. Dercz, M. Zubko, J. Maszybrocka, J. Jurek-Suliga, S. Golba, I. Jendrzejewska, Microstructure and porosity evolution of the Ti–35Zr biomedical alloy produced by elemental powder metallurgy, Materials **13** (20), 1532 (2020). DOI: https://doi.org/10.3390/ma13204539

[11] T.B. Massalski, H. Okamoto, P.R. Subramanian, B. Massalski, L. Thaddeus, Binary Alloy Phase Diagrams, 2nd Editio, ASM International, 1990.

[12] J. Breme, V. Wadewitz, Comparison of titanium-tantalum and titanium-niobium alloys for application as dental implants, Int. J. Oral Maxillofac. Implants. **4**, 113-118 (1989).

[13] Y. Guo, K. Georgarakis, Y. Yokoyama, A.R. Yavari, On the mechanical properties of TiNb based alloys, J. Alloys Compd. **571**, 25-30 (2013). DOI: https://doi.org/10.1016/j.jallcom.2013.03.192

[14] J.M. Cordeiro, T. Beline, A.L.R. Ribeiro, E.C. Rangel, N.C. da Cruz, R. Landers, L.P. Faverani, L.G. Vaz, L.M.G. Fais, F.B. Vicente, C.R. Grandini, M.T. Mathew, C. Sukotjo, V.A.R. Barão, Development of binary and ternary titanium alloys for dental implants. Dent. Mater. **33**, 1244-1257 (2017). DOI: https://doi.org/10.1016/j.dental.2017.07.013

[15] D. Kuroda, M. Niinomi, M. Morinaga, Y. Kato, T. Yashiro, Design and mechanical properties of new i type titanium alloys for implant materials, Mater. Sci. Eng. A **243**, 244-249 (1998).

[16] S. Miyazaki, K. Otsuka, Development of Shape Memory Alloys, ISIJ Int. **29**, 353-377 (1989). DOI: https://doi.org/10.2355/isijinternational.29.353

[17] D.B. Wiles, R.A. Young, A new computer program for Rietveld analysis of X-ray powder diffraction patterns, J. Appl. Cryst. **14**, 149-151 (1981).

[18] H.M. Rietveld, A Profile Refinement Method for Nuclear and Magnetic Structure, J. Appl. Cryst. **3**, 65-69 (1969).

[19] R.A. Young, The Rietveld method, 1993, Oxfor Univ. Press.

[20] C.M. Lee, C.P. Ju, J.H. Chern Lin, Structure-property relationship of cast Ti-Nb alloys, J. Oral Rehabil. **29**, 314-322 (2002). DOI: https://doi.org/10.1046/J.1365-2842.2002.00825.X

[21] A.I. Mardare, A. Savan, A. Ludwig, A.D. Wieck, A.W. Hassel, A combinatorial passivation study of Ta-Ti alloys, Corros. Sci. **51**, 1519-1527 (2009). DOI: https://doi.org/10.1016/J.CORSCI.2008.12.003

[22] G. Dercz, I. Matuła, M. Zubko, A. Kazek-Kęsik, J. Maszybrocka, W. Simka, J. Dercz, P. Świec, I. Jendrzejewska, Synthesis of porous Ti-50Ta alloy by powder metallurgy, Mater. Charact. **142**, 124-136 (2018). DOI: https://doi.org/10.1016/j.matchar.2018.05.033

[23] W.F. Ho, W.K. Chen, S.C. Wu, H.C. Hsu, Structure, mechanical properties, and grindability of dental Ti-Zr alloys, J. Mater. Sci. Mater. Med. **19**, 3179-3186 (2008). DOI: https://doi.org/10.1007/s10856-008-3454-x

[24] M. Takahashi, M. Kikuchi, O. Okuno, Grindability of Dental Cast Ti-Zr Alloys, Mater. Trans. **50** (4), 859-863 (2009). DOI: https://doi.org/10.2320/matertrans.MRA2008403

[25] M. Abdel-Hady, H. Fuwa, K. Hinoshita, H. Kimura, Y. Shinzato, M. Morinaga, Phase stability change with Zr content in B-type Ti-Nb alloys, Scr. Mater. **57**, 1000-1003 (2007). DOI: https://doi.org/10.1016/j.scriptamat.2007.08.003

[26] M. Abdel-Hady Gepreel, M. Niinomi, Biocompatibility of Ti-alloys for long-term implantation, J. Mech. Behav. Biomed. Mater. **20**, 407-415 (2013). DOI: https://doi.org/10.1016/j.jmbbm.2012.11.014

[27] G. Dercz, I. Matuła, M. Zubko, J. Dercz, Phase composition and microstructure of new Ti-Ta-Nb-Zr biomedical alloys prepared by mechanical alloying method, Powder Diffr. **32**, S186-S192 (2017). DOI: https://doi.org/10.1017/S0885715617000045

[28] S. Ozan, J. Lin, Y. Li, C. Wen, New Ti-Ta-Zr-Nb alloys with ultrahigh strength for potential orthopedic implant applications, J. Mech. Behav. Biomed. Mater. **75**, 119-127 (2017). DOI: https://doi.org/10.1016/j.jmbbm.2017.07.011

[29] X. Tang, T. Ahmed, H.J. Rack, Phase transformations in Ti-Nb-Ta and Ti-Nb-Ta-Zr alloys, J. Mater. Sci. **35**, 1805-1811 (2000). DOI: https://doi.org/10.1023/A:1004792922155